IRIS

INSTITUTIONAL RESEARCH INFORMATION SYSTEM
ARCHIVIO ISTITUZIONALE DEI PRODOTTI DELLA RICERCA

intestazione repositorydell'ateneo

miRNA-mRNA integrative analysis in primary myelofibrosis CD34+ cells: role of miR-155/JARID2 axis in abnormal megakaryopoiesis

18 September 2017

miRNA-mRNA integrative analysis in primary myelofibrosis CD34+ cells unveils the role of miR-155/JARID2 axis in abnormal megakaryopoiesis

Short Title: Integrative analysis of miRNA-mRNA in PMF cells

Ruggiero Norfo[1]*, Roberta Zini[1]*, Valentina Pennucci[1]*, Elisa Bianchi[1], Simona Salati[1], Paola Guglielmelli[2], Costanza Bogani[2], Tiziana Fanelli[2], Carmela Mannarelli[2], Vittorio Rosti[3], Daniela Pietra[4], Silvia Salmoiraghi[5], Andrea Bisognin[6], Samantha Ruberti[1], Sebastiano Rontauroli[1], Giorgia Sacchi[1], Zelia Prudente[1], Giovanni Barosi[3], Mario Cazzola[4], Alessandro Rambaldi[5], Stefania Bortoluzzi[6], Sergio Ferrari[7], Enrico Tagliafico[7], Alessandro M. Vannucchi[2]# and Rossella Manfredini[1]#¶ on behalf of the AGIMM (AIRC Gruppo Italiano Malattie Mieloproliferative) investigators

*equal contribution
AMV and RM share senior authorship

[1]Centre for Regenerative Medicine, Department of Life Sciences, University of Modena and Reggio Emilia, Modena, Italy; [2]Department of Experimental and Clinical Medicine, University of Florence, Florence, Italy; [3]Center for the Study of Myelofibrosis, IRCCS Policlinico S.Matteo Foundation, Pavia, Italy; [4]Department of Hematology Oncology, IRCCS Policlinico San Matteo Foundation & University of Pavia, Pavia, Italy; [5]Hematology, Az. Osp. Papa Giovanni XXIII, Bergamo, Italy; [6]Department of Biology, University of Padua, Padua, Italy; [7]Center for Genome Research, Department of Life Sciences, University of Modena and Reggio Emilia, Modena, Italy

¶Corresponding author: Rossella Manfredini, PhD, Centre for Regenerative Medicine

"Stefano Ferrari", University of Modena and Reggio Emilia, via Gottardi n.100, 41125

Modena, Italy. E-mail: rossella.manfredini@unimore.it

Scientific Category: Myeloid Neoplasia

1

Key points:

- Differential gene and miRNA expression analysis in PMF granulocytes identifies new biomarkers and putative therapeutic targets

- Activation of miR-155/*JARID2* axis in PMF CD34+ cells results in overproduction of megakaryocyte precursors

ABSTRACT

Primary myelofibrosis (PMF) is a myeloproliferative neoplasm characterized by megakaryocyte hyperplasia, bone marrow fibrosis, and abnormal stem cell trafficking. PMF may be associated with somatic mutations in *JAK2*, *MPL*, or *CALR*. Previous studies have shown that abnormal megakaryocytes play a central role in the pathophysiology of PMF. In this work, we studied both gene and microRNA (miRNA) expression profiles in CD34+ cells from PMF patients. We identified several biomarkers and putative molecular targets such as *FGR*, *LCN2*, and *OLFM4*. By means of miRNA-gene expression integrative analysis, we found different regulatory networks involved in the dysregulation of transcriptional control and chromatin remodeling. In particular, we identified a network gathering several oncomiRs (e.g., miR-155-5p) and targeted genes whose abnormal function has been previously associated to myeloid neoplasms, including *JARID2*, *NR4A3*, *CDC42*, and *HMGB3*. Since the validation of miRNA-target interactions unveiled *JARID2*/miR-155-5p as the strongest relationship in the network, we studied the function of this axis in normal and PMF CD34+ cells. We showed that *JARID2* downregulation mediated by miR-155-5p overexpression leads to increased in vitro formation of CD41+ megakaryocyte precursors. These findings suggest that overexpression of miR-155-5p and the resulting downregulation of *JARID2* may contribute to megakaryocyte hyperplasia in PMF.

INTRODUCTION

Philadelphia-negative chronic myeloproliferative neoplasms (MPNs) are a heterogeneous group of clonal hematopoietic stem cell disorders associated with overproduction of mature myeloid cells, and include primary myelofibrosis (PMF)[1,2]. The molecular mechanisms underlying MPN pathogenesis were partially disclosed in 2005–2006 with the identification of somatic gain-of-function mutations of *JAK2* and *MPL*[3,4], after which many other mutated genes were found[5,6], such as *CALR*[7,8]. Despite the fact that the mutational landscape of MPNs has been extensively investigated, a comprehensive framework of the pathogenetic molecular mechanisms has not been fully elucidated.

MicroRNAs (miRNAs) are small non-coding RNAs involved in several biological processes such as differentiation[9], proliferation[10], and apoptosis[11] through the post-transcriptional repression of their targets[12]. Increasing evidence shows that deregulation of miRNAs plays an important role in both solid and hematologic malignancies[13,14]. In particular, recent reports pointed to aberrant miRNA expression in MPNs, and specific miRNA signatures that distinguish MPN granulocytes from those of healthy donors have been described[15,16]. However, because MPNs are stem cell-derived disorders, studies on disease mechanisms should be focused on a more primitive cell compartment. High-throughput analysis of miRNA expression levels in MPN CD34+ cells has been reported in only two studies, including a limited number of patients[17,18]; therefore, our understanding of miRNAs' involvement in MPN pathogenesis is still limited.

Here, we focused our attention on the molecular mechanisms underlying PMF, the less common, and likely the most pathogenetically complex of the MPNs. In order to define the role of miRNAs in the pathogenesis of PMF, we obtained both miRNA and gene expression profiles (miEP and GEP, respectively) in the same sample of CD34+ cells from 42 PMF patients and 31 healthy donors. Integration of these profiles allowed us to unveil how differentially expressed miRNAs (DEMs) potentially influence the dysregulation of several biological processes in PMF by interacting with their target genes.

In particular, we described a regulatory network involving several upregulated oncomiRs and their target mRNAs, including *CDC42*, *HMGB3* and *NR4A3* that were previously characterized in knockout murine models of myeloproliferative disorders, and the chromatin remodeler *JARID2*.

We also demonstrated that miR-155-5p affects the *in vitro* expansion of the megakaryocyte (MK) lineage through the modulation of *JARID2* expression, suggesting

4

that the miR-155-5p*/JARID2* axis might contribute to the abnormal megakaryopoiesis typical of PMF.

MATERIALS AND METHODS

Patients and samples

Forty-two patients with a diagnosis of PMF in a typical fibrotic stage of the disease according to the World Health Organization (WHO)[19] were included in the microarray analysis. Their characteristics are reported in **Table S1**. PMF CD34+ cells were purified from peripheral blood (PB). In addition, 16 PB samples and 15 bone marrow (BM) samples were collected from normal donors. Moreover, an independent cohort of 36 PMF patients, 12 healthy donors, and 26 cord blood (CB) samples was selected for validation studies.

All subjects provided informed written consent, and the study was performed under the local Institutional Review Board's approved protocol. The study was conducted in accordance with the Declaration of Helsinki.

The presence of the *JAK2*V617F mutation and the allele burden were determined via quantitative reverse transcription polymerase chain reaction (qRT-PCR), as previously described[20].

GEP and miEP integrative analysis

GEP and miEP were performed on the same RNA preparation using the Affymetrix technology (HG-U219 Array Strip and miRNA 2.0 arrays) as detailed in the Supplemental Methods.

Differentially expressed genes (DEGs) and miRNAs (DEMs) were then selected following a supervised approach with the ANOVA module included in the Partek GS package. In particular, we selected all the probe sets with a fold change contrast ≥2 for DEGs, or ≥1.5 for DEMs in the pairwise comparison of PMF versus controls, and a false discovery rate (FDR) (q-value) <.05.

To construct the regulatory networks of the functional miRNA-target interactions, *in silico* integrative analysis (IA) was performed by using Ingenuity Pathway analysis software (IPA, version 8.6; Ingenuity Systems; Redwood City, CA, http://www.ingenuity.com), which combines computationally predicted targets with gene expression data. Briefly, the lists of DEMs and DEGs were separately uploaded on the software; then, the putative targets of DEMs were identified within the DEG list by microRNA Target Filter, according to at least one out of four different databases (TargetScan, miRecords, Tarbase, or Ingenuity expert findings); finally, pairs with anti-correlated expression trends were filtered and selected for further analysis to build the regulatory networks.

Electroporation of CD34+ cells

The electroporation program of CD34+ cells was based on a previously published protocol[21], which was optimized to be performed on the 4D-Nucleofector™ System (Lonza) (see Supplemental Results). Briefly, each sample was electroporated three times once every 24 hours (h) with a mix of three Silencer Select small interfering RNAs (siRNAs) targeting human *JARID2* (**Table S2**) (Life Technologies), starting from the day after CD34+ cell purification[22]. For each electroporation, 4×10^5 CD34+ cells were resuspended in 100 µL of P3 Primary Cell Solution (Lonza), containing 3 µg of siRNA mix, and pulsed with the program DS112. To exclude non-specific effects caused by interfering RNA (RNAi) nucleofection, a sample transfected with a non-targeting siRNA (NegCTR; Silencer Select Negative Control #2 siRNA; Life Technologies) was included.

As described for siRNA transfections, the number of nucleofections and the quantities of miRNA mimics/inhibitors were modified from a previously described protocol[23] to best fit the properties of the second generation of miRNA mimics/inhibitors (Life Technologies). Briefly, CD34+ cells were nucleofected twice, once every 24 h, with 3 µg of mirVana™ miR-155-5p mimic or mirVana™ miRNA mimic Negative Control #1 (Neg-mimic), by using the above-mentioned electroporation protocol DS112. PMF and CB CD34+ cells were nucleofected four times, once every 24 h, with 3 µg of mirVana™ miR-155-5p inhibitor or mirVana™ miRNA inhibitor Negative Control #1 (NegINH), by using the electroporation protocol DS112.

Cells were analyzed 24 h and 48 h after the last nucleofection for both cell viability and *JARID2* or miR-155-5p expression.

Statistical analysis

The SPSS software (StatSoft; Tulsa) was used for statistical analysis of clinical correlation. Comparison between groups was performed by using the Student's *t*-test, and the chosen level of significance was $P < .05$ with a two-sided test.

The statistics used for data analysis in silencing/overexpression experiments and 3´UTR luciferase reporter assays were based on two-tailed Student's *t*-tests for averages comparison in paired samples. Data were analyzed by using Microsoft Excel (Microsoft Office, 2008 release) and are reported as mean ± standard error of the mean (SEM). $P < .05$ was considered significant.

RESULTS

Gene expression profile of CD34+ cells from PMF patients

We performed mRNA expression profiling in CD34+ cells from 42 PMF patients (n=23 JAK2V617F-positive, n=19 wild-type JAK2) and 31 healthy donors (n=15 from the BM and n=16 from the PB). All microarray data (GEP and miEP) were submitted to the Gene Expression Omnibus repository (GEO; http://www.ncbi.nlm.nih.gov/geo) and can be downloaded as series GSE41812 and GSE53482.

After data pre-processing, to explore the relationships between samples, we performed a principal component analysis (PCA). **Figure 1A** shows that the PMF samples clustered together and were clearly separated from both the BM and PB control samples. Of note, unsupervised analysis was unable to ungroup JAK2V617F and wild-type JAK2 patients.

Next, using an analysis of variance (ANOVA)-based supervised approach for comparing PMF samples with both BM and PB controls, we identified 718 DEGs. **Table S3** shows the 100 most up- and downregulated genes.

Array data confirmed the abnormal expression of several genes (i.e., *WT1*, *NFE2*, *CXCR4*, *CD9*) previously identified as deregulated in PMF CD34+ cells by our group in a different cohort of PMF patients[24]. Moreover, PMF samples exhibited increased levels of several putative cancer markers, such as *ANGPT1*, *CEACAM8*, and *CP*, previously reported to be associated with poor prognosis in hematological and solid neoplasms, as well as genes associated with BM fibrosis (*LEPR*, *MMP9*, and *TIMP3*) and aberrant migration (*TM4SF1*, *RHOB*, *ARHGAP18*, and *MMP8*). In addition, PMF samples showed a deregulated expression pattern of a number of transcription factors and chromatin remodelers involved in myeloid and MK commitment, either downregulated (i.e., *JARID2*, *RUNX2*, *KLF3*, and *AFF3*) or upregulated (i.e., *FHL2*, *MAF*, and *IKZF2)* (for a list of pertinent references, see **Table S4**). A selected list of DEGs chosen for their biological significance is presented in **Table 1**.

To validate the array data, we designed a TaqMan low-density array containing 63+*GAPDH* TaqMan gene expression assays (**Table S5**). The selection of genes was based on either the highest absolute fold change contrast and/or their putative role in PMF pathogenesis. TaqMan assays were carried out in an independent cohort of CD34+ cells from 10 PMF patients and 8 healthy subjects (n=4 BM, n=4 PB) and enabled validation of the expression of 50 out of 63 genes (79.4%) (**Table S6**).

miRNA expression profile of CD34+ cells from PMF patients

To draw a comprehensive picture of miRNA deregulation and its relationship with differential gene expression in PMF cells, we performed miEP in the same sample set, using the Affymetrix miRNA 2.0 arrays. As already described for GEP, after an initial pre-processing of data aimed at removing the noise, we performed a PCA to explore the relationships between samples. **Figure 1B** depicts the PCA graph, which shows the presence of a cluster of PMF samples that is clearly distinct from the PB and BM samples; moreover, PCA did not show any difference between mutated JAK2V617F and wild-type JAK2 patients, similar to the GEP PCA.

Next, by using an ANOVA-based supervised approach as described in the Methods section, we selected 76 DEMs (**Table S7**). In particular, we found several upregulated miRNAs associated with hematological malignancies, or known as oncomiRs (i.e., miR-155-5p, miR-21-5p, miR-29a-3p, and miRNAs belonging to the miR-17-92 cluster)[25]. By contrast, among the downregulated miRNAs, we found miR-378c, which is described as a tumor suppressor gene in gastric cancer[26]. Furthermore, overexpressed miRNAs previously identified as being involved in MK commitment were also found (i.e., miR-146b-5p and miR-34a-5p)[27].

To validate the array data, we used TaqMan single microRNA assays to assess the expression of 46 DEMs, which were selected based on either their relatively high differential expression or their biological role in cancer-related processes or myeloid differentiation (**Table S8**). TaqMan assays were carried out in an independent cohort of CD34+ cells from 10 PMF patients and 8 healthy subjects (n=4 BM, n=4 PB) and confirmed the deregulated expression of 34 out of 46 miRNAs (73.9%) (**Table S9**).

Validation of a gene set on granulocytes and serum from PMF patients

Among the 50 validated genes described above, we selected a set of 7 genes (*OLFM4*, *LCN2*, *LEPR*, *FGR*, *ANXA3*, *CEACAM8*, and *DEF1A*) out of those most upregulated to validate their expression in granulocytes, which represent a more appropriate source for diagnostic/prognostic purposes. Using qRT-PCR, we observed that *OLFM4*, *LCN2*, *LEPR*, *FGR*, and *ANXA3* mRNA levels were significantly increased in PMF granulocytes (n=32) compared to healthy controls (n=12) (**Figure 2A**), whereas *CEACAM8* and *DEF1A* expression was not statistically modulated between the two groups (data not shown).

Since *OLFM4* and *LCN2* genes encode for two secreted proteins, we assessed OLFM4 and LCN2 protein levels in the serum of the same PMF patients (n=32) and healthy donors

(n=8) by means of an enzyme-linked immunosorbent assay (ELISA). As shown in **Figure 2B**, the levels of OLFM4 and LCN2 secreted proteins were significantly higher in PMF patients than in healthy donors. Of note, the median concentration of OLFM4 serum protein was 5-fold higher in PMF patients than in controls.

Validation of the selected miRNAs in the granulocytes from PMF patients

Among the validated miRNAs in PMF CD34+ cells, we selected the 16 most upregulated ones (**Table S9**) to test their expression in the granulocytes from the same PMF patients (n=30) and healthy donors (n=8) previously used for mRNA expression validation. We demonstrated that the levels of miR-19a-3p, miR-335-5p, miR-379-5p, miR-376c-3p, miR-487b-3p, and miR-494-3p were significantly increased in PMF granulocytes compared with controls, whereas miR-486-3p expression was significantly decreased in PMF granulocytes, in contrast to the results obtained in CD34+ cells (**Figure 2C**). The levels of the remaining miRNAs were not statistically modulated between PMF and controls (data not shown).

GEP and miEP integrative analysis

Since each miRNA can target many mRNAs while a single mRNA can be targeted by multiple miRNAs, we performed IA by means of IPA to untangle this combinatorial complexity. Based on IPA, we selected DEM-DEG pairs with an anti-correlated expression pattern. In particular, 56 out of the 76 DEMs have at least one anti-correlated target among DEGs, whereas 445 out of the 718 DEGs have at least one anti-correlated targeting DEM. 1167 anti-correlated miRNA-target pairs were finally generated.

Among the interaction networks uncovered by IPA, we focused our attention on three of them because of their enrichment in genes and miRNAs involved in myeloproliferative disorders and/or in hematopoietic differentiation. **Figure 3A** shows several miRNAs that are highly expressed in PMF, such as miR-18a-5p, miR-29a-3p, miR-433-3p, miR-19a-3p, miR-155-5p, miR-195-5p, miR-200c-3p, and miR-152-3p, and their downregulated targets (*BRWD1*, *JARID2*, *PHC3*, and *HMGB3*) implicated in chromatin remodeling, a process severely impaired in MPNs. The second network (**Figure 3B**) displays several upregulated miRNAs involved in myeloid differentiation (miR-155-5p, miR-21-5p, miR-29a-3p)[28] and their interactions with downregulated transcription factors, known as leukemic tumor suppressors (*TLE4*, *MLL5*, *FOXO1*) or myeloid commitment regulators (*CEBPD*, *CEBPG*, *MAFF*, *TCF4*, *MXD1*).

Finally, through IA we could identify a regulatory network gathering a high number of upregulated oncomiRs (i.e., miR-155-5p, miR-29a-3p, miR-92b-3p, miR-19a-3p, miR-18a-5p) targeting anti-correlated mRNAs whose downregulation or deletion has been related to hematopoietic disorders. In particular, hypoallelic *NR4A3* or *CDC42* knockout in mice leads to a myeloproliferative disorder[29,30], while *JARID2* is a frequently deleted gene in leukemic transformation of chronic myeloid malignancies[31]; the other target *HMGB3* is instead described as a regulator of self-renewal/differentiation balance in murine hematopoietic stem cells[32] (**Figure 3C**).

miRNA-mRNA interaction validation by luciferase reporter assays

Because the network shown in **Figure 3C** contained the highest number of oncomiRs and targets involved in malignant hematopoiesis, it was selected to validate every putative miRNA/target pair by assessing 3′ untranslated region (UTR) luciferase activity upon miRNA overexpression; K562 cells were selected as *in vitro* system providing a hematopoietic background. As shown in **Figure 4A**, our data demonstrated that the following 3′UTR-miRNA interactions were statistically significant: JARID2 3′UTR- by miR-152-3p, miR-195-5p, and miR-155-5p (further details on JARID2 3′UTR/miR-155-5p interaction are provided in the Supplemental Results); CDC42 3′UTR- by miR-29a-3p and miR-18a-5p; HMGB3 3′UTR- by miR-152-3p, miR-200c-3p, miR-433-3p, and miR-155-5p; NR4A3 3′UTR- by miR-335-5p and miR-92b-3p. Conversely, the interactions between the remaining miRNA-3′UTR target pairs were not confirmed. **Figure 4B** graphically recapitulates all the confirmed and non-confirmed interactions of the IA network previously shown. **Figure 4C** clearly shows that mutations in the miRNA binding site of 3'UTR targets prevented the decrease in luciferase reporter activity by miRNAs, which conversely occurs in their wild-type counterparts. Collectively, the luciferase assay data support the good predictive power by IA, as demonstrated by the 11/17 (64.7%) successful predictions for the selected network.

Silencing of JARID2 in normal CD34+ cells

Since the contribution of *JARID2* to PMF pathogenesis has never been investigated, we performed RNAi-mediated gene silencing experiments on normal CD34+ cells. First, we optimized the CD34+ cell nucleofection protocol for the Amaxa 4D-Nucleofector™ System technology (see Supplemental Results).

CD34+ cells were transfected with a mixture of three Silencer Select siRNAs targeting *JARID2* mRNA (**Table S2**) and with a non-targeting siRNA as a negative control (NegCTR). The expression level of *JARID2* in control samples and *JARID2*-siRNA cells was assessed by qRT-PCR at 24 and 48 h after the last nucleofection (**Figure 5A**).

Flow cytometric analysis of the CD41 MK marker performed on serum-free multilineage culture at day 8, 10, and 12 showed that *JARID2* inhibition induces a significant increase in the MK fraction compared to the NegCTR sample (**Figure 5B**). Unilineage MK differentiation culture experiments further confirmed these results (**Figure 5C**). Flow cytometric analysis of granulocytic, mono-macrophagic, and erythrocyte differentiation markers did not highlight any significant modulation between *JARID2*-siRNA CD34+ cells and the NegCTR sample (data not shown). The methylcellulose assay indicated a 1.5-fold increase in the clonogenic efficiency of *JARID2*-siRNA CD34+ cells versus the NegCTR sample, whereas there was no significant difference in the percentage of erythroid and myeloid colonies (data not shown).

Next, we examined the effect of *JARID2* silencing on MK commitment by plating NegCTR and *JARID2*-siRNA CD34+ cells in a collagen-based serum-free semisolid culture medium that supports the growth of MK progenitors *in vitro*. The results, reported in **Figure 5D**, demonstrated that *JARID2* silencing induces a remarkable increase in colony-forming unit-megakaryocytes (CFU-MK) and a strong decrease of non-megakaryocyte colonies (CFU non-MK) compared to the NegCTR sample. Moreover, morphological evaluation of May–Grünwald–Giemsa-stained (MGG-stained) cytospins of thrombopoietin-treated cells at day 8 and 10 after the last nucleofection clearly displayed a considerable enrichment in MK precursors at different stages of maturation in *JARID2*-siRNA cells compared to NegCTR (**Figure 5E**). Finally, to better characterize the changes in gene expression induced by *JARID2* gene silencing, we performed mRNA profiling in NegCTR and *JARID2*-siRNA CD34+ cells (see Supplemental Results and **Figure S1**).

miR-155-5p overexpression and silencing in normal and PMF CD34+ cells

Next, we asked whether any *JARID2*-targeting miRNA could reproduce its silencing effects on MK differentiation. Thus, we decided to overexpress miR-155-5p in normal CD34+ cells, because it was highlighted by the luciferase reporter assay as the strongest regulator of the *JARID2* 3´UTR (**Figure 4A**). Furthermore, a significant negative correlation was observed between miR-155-5p and *JARID2* expression levels across the whole microarray dataset (r= –0.55, *P*=5.29×10^{-7}) (**Figure S2**).

CD34+ cells were transfected either with miR-155-5p mimic or with Neg-mimic. By means of qRT-PCR, we observed that the *JARID2* mRNA level was downregulated upon miR-155-5p overexpression (RQ±SEM, 34.7±11.1, *P* < .05) at 24 and 48 h after the last nucleofection (**Figure 6Ai**).

As observed for the *JARID2* knockdown, miR-155-5p overexpression led to a significant increase of the percentage of CD41+ cells at day 10 and 12 after the last nucleofection in serum-free multi-lineage culture (**Figure 6Aii**). Similar results were obtained under unilineage MK differentiation culture conditions (**Figure 6Aiii**). Furthermore, the collagen-based assay showed that miR-155-5p overexpression causes a significant increase in the CFU-MK percentage coupled with a strong decrease of non-MK colonies (**Figure 6Aiv**). Finally, the morphological analysis of MGG-stained cytospins showed a remarkable enrichment in MK precursors at different stages of maturation in miR-155-5p–overexpressing cells compared to controls at day 10 and 12 after the last nucleofection (**Figure 6Av**).

Furthermore, we aimed at assessing whether miR-155-5p downregulation in PMF CD34+ cells could reduce the expansion MK lineage. First, we evaluated *JARID2* levels upon miR-155-5p silencing, observing a statistically significant increase at 24 and 48 h after the last nucleofection (**Figure 6Bi**). Strikingly, knockdown of miR-155-5p impaired the ability of PMF CD34+ cells to give rise to CD41+ cells, in both multi-lineage and MK unilineage cultures (**Figure 6Bii-iii**). Those observations were further confirmed by decrease of CFU-MK colonies in collagen-based assays (**Figure 6Biv**) and by decrease of MK progenitors in MGG-stained cytospins (**Figure 6Bv**).

Functional validation of the miR-155-5p/*JARID2* axis in MK lineage expansion

In order to demonstrate that miR-155-5p affects megakaryocytopoiesis by means of *JARID2* modulation, we concurrently overexpressed *JARID2* and miR-155-5p in normal CD34+ cells. To this aim, CB CD34+ cells were nucleofected twice with miR-155-5p or Neg-mimic and consecutively transduced with the retroviral vector expressing JARID2 cDNA (LJARID2IΔN) or empty vector (LXIΔN) (see timing flowchart in **Figure 7Ai** and Supplemental Methods)[33]. To assess *JARID2* expression, qRT-PCR was performed after NGFR+ cell purification (**Figure 7Aii**). As shown in **Figure 7Aiii,** the fraction of CD41+ cells in the MK unilineage culture decreased in miR-155-5p/LJARID2IΔN compared to miR-155-5p/LXIΔN cells at day 4, 7, and 11 post-purification. Moreover, the CFU-MK

assay results showed that *JARID2* overexpression in miR-155-5p cells causes a significant decrease in the CFU-MK percentage compared to miR-155-5p/LXIΔN cells (**Figure 7Aiv**). Furthermore, to confirm that miR-155-5p driven megakaryopoiesis depends on *JARID2* mRNA levels, we simultaneusly silenced miR-155-5p and *JARID2* in normal CD34+ cells (see timing flowchart in **Figure 7Bi** and Supplemental Methods). The expression level of *JARID2* was assessed by qRT-PCR at 48 h after the last nucleofection (**Figure 7Bii**). Flow cytometric analysis of CD41 expression performed on the MK unilineage culture at day 8, 10, and 12 after the last nucleofection showed a decrease in the MK fraction in miR-155-5p-silenced cells compared to NegCTR/NegINH cells (**Figure 7Biii**). As expected, the simultaneous *JARID2* knockdown could rescue the MK differentiation unbalance in miR-155-5p silenced cells. In agreement with the flow cytometry data, the results of MK assay highlighted that the concurrent downregulation of miR-155-5p and *JARID2* could prevent the impairment of MK differentiation observed in both independently silenced miR-155-5p and *JARID2* samples (**Figure 7Biv**).

DISCUSSION

In this study, we aimed at characterizing the role of miRNAs in PMF pathogenesis. To this end, we integrated GEP and miEP of PMF CD34+ cells, demonstrating how differentially expressed miRNAs affect the gene expression pattern in PMF cells. In particular, miRNA-mRNA expression data integration led to the identification of several networks, one of which was further investigated in terms of interactions between miRNAs and the 3´UTRs of their putative targets. Finally, we demonstrated that the overexpression of miR-155-5p in normal CD34+ cells, as well as the silencing of its validated target *JARID2*, determines the expansion of the megakaryocytic lineage. Conversely, we showed that miR-155-5p inhibition in PMF CD34+ cells impaired the MK commitment. Overall, this work sheds light on the influence of deregulated miRNAs on gene expression regulation in PMF CD34+ cells and on their contribution to features typical of PMF, such as a hyperplastic megakaryopoiesis. In parallel, the assessment of the expression levels of several DEGs in PMF granulocytes highlighted a number of possible disease markers, which might eventually become relevant for target therapy approaches, such as membrane protein- and kinase-coding genes.

Because miRNAs were recently demonstrated to be deregulated in MPN cells[15-17], interest of their involvement in pathogenetic mechanisms is progressively growing. However, most of the miRNA and mRNA expression studies performed to date have been conducted using terminally differentiated hematopoietic cells, namely granulocytes or megakaryocytes[15,16,34,35]. Since MPNs are considered to arise from the hematopoietic stem cell compartment[36], understanding of the pathogenetic molecular mechanisms should best be assessed by studying CD34+ cells. So far, only two studies have reported data on miRNA expression profiling in a very small number of MPN CD34+ samples[17,18], and no integrated miRNA-mRNA expression analysis was available until now. Here, we provide the results of an extensive study that profiled both gene and miRNA expression in the same CD34+ cell sample from 42 PMF patients.

GEP and miEP analysis showed that PMF CD34+ cells present a different expression pattern compared to BM and unmobilized PB CD34+ cells; of note, PCA was unable to separate PMF patients according to JAK2 mutational status (**Figures 1A and B**). Differential expression analysis enabled the identification of several deregulated miRNAs and mRNAs suitable as biomarkers or as putative molecular targets for diagnostic or prognostic purposes. Therefore, the most upregulated genes and miRNAs were monitored on PMF granulocytes because they could represent a more suitable cell source for clinical

praxis, whereas secreted protein levels were assessed in the patients' sera. We identified a set of five genes (i.e., *LCN2*, *OLFM4*, *ANXA3*, *FGR*, and *LEPR*) (**Figure 2A**) and six miRNAs (i.e., miR-19a-3p, miR-335-5p, miR-376c-3p, miR-379-5p, miR-487b-3p, and miR-494-3p) (**Figure 2B**) whose expression levels are aberrant in PMF granulocytes as well as in CD34+ cells. Evidence in PMF of a higher mRNA expression of the leptin receptor (*LEPR*), previously reported in AML[37], as well as of Src kinase *FGR*[38], could also be useful to drive the future design of targeted drugs. Of note, LEPR and Src kinase inhibitors are already being used in preclinical or clinical trials[39,40]. In addition, we demonstrated that OLFM4 and LCN2 secreted protein levels could be considered as PMF biomarkers, since they were significantly high in patients' sera compared to those of healthy controls. Strikingly, more than 80% of the PMF patients presented with higher OLFM4 protein levels compared to all the evaluated controls.

The present study has mainly provided information about the molecular mechanisms underlying PMF pathogenesis. Indeed, data analysis clearly showed that several genes involved in adhesion or migration processes (*TM4SF1*, *RHOB*, *ARHGAP18*, and *MMP8*) as well as fibrogenic potential (*LEPR*, *MMP9,* and *TIMP3*) are deregulated in PMF CD34+ cells. Interestingly, regulators of megakaryocytic commitment were also upregulated (i.e., *NFE-2*, *MEF2C*, miR-146b-5p, miR-34a-5p). Furthermore, we found an increased expression of genes or miRNAs with oncogenic potential, i.e., *CEACAM8*, *ANGPT1*, miR-29a-3p, and miRNAs belonging to the miR-17-92 cluster [25,41] (**Table S4**).

Since one of the main mechanisms through which miRNAs act is degradation of specific targets[42], miRNAs and their targets are expected to display anti-correlated expression. Hence, we performed IA to select more reliable interactions among those predicted *in silico*. As chromatin remodeling is one of the main processes involved in PMF pathogenesis, we determined whether a DEM could affect this pathway. **Figure 3A** shows that chromatin remodeler genes such as *PHC3* and *HMGB3* could be downregulated by a network of upregulated targeting miRNAs, i.e., miR-18a-5p, miR-433-3p, miR-195-5p, miR-200c-3p, and miR-152-3p. We also observed that low expression of different hematopoietic transcription factors as well as leukemia suppressors (i.e., *CEBP*, *FOXO1*, *MLL5*) is, at least in part, caused by several highly expressed oncomiRs such as miR-21-5p and miR-29a-3p, as depicted in **Figure 3B**. Finally, a single regulatory network collecting the highest number of oncomiRs and target genes involved in malignant hematopoiesis is shown in **Figure 3C**. Of note, by means of 3´UTR luciferase reporter assays, we were able to confirm 11/17 (64.7%) putative interactions for the above-

mentioned network, highlighting the good predictive power of IA in identifying true miRNA-target interactions (**Figure 4**). Specifically, the upregulation of several targeting miRNAs explains the negative regulation of genes like *CDC42* and *NR4A3*, whose downregulation leads to myeloproliferative disorders in murine models[29,30], as well as *HMGB3*, which codes for a regulator of the self-renewal/differentiation balance in murine hematopoietic stem cells[32]. Moreover, upregulated miR-155-5p, miR-195-5p, and miR-152-3p share the experimentally observed target *JARID2*, a chromatin remodeler that is a member of the Jumonji family of transcription factors belonging to the polycomb repressive complex 2 (PRC2)[43]. Of note, Puda and colleagues demonstrated that *JARID2* is frequently deleted in leukemic transformation of chronic myeloid malignancies[31]. However, although the function of *JARID2* in hematopoiesis has been already partially unraveled in mouse embryo development studies, there are no data about its role in human primary hematopoietic CD34+ cells[44]. Thus, we decided to investigate the effect of *JARID2* downregulation in hematopoiesis by means of RNAi-mediated silencing in human normal CD34+ cells. Our findings support the contributing role of *JARID2* deficiency in the expansion of the MK lineage both in liquid and in semisolid culture, as shown in **Figure 5**. Because the most effective miRNA in downregulating JARID2 3′UTR-luciferase activity was miR-155-5p, whose enforced expression causes a myeloproliferative disorder in mice[45], we accordingly overexpressed this miRNA in hematopoietic CD34+ cells. Here, we demonstrated that miR-155-5p overexpression downregulates *JARID2* mRNA, thus supporting the expansion of the MK compartment (**Figure 6A**). In parallel, miRNA inhibition in PMF CD34+ cells clearly showed that miR-155-5p may play an important role in the increased megakaryopoiesis observed in PMF patients (**Figure 6B**). Finally, the restoration of *JARID2* expression level in miR-155-5p-overexpressing CD34+ cells impaired the expansion of MK lineage induced by miR-155-5p (**Figure 7A**); this unbalance could be prevented by simultaneously silencing *JARID2* and miR-155-5p as well, thus definitively demonstrating that miR155-5p affects megakaryopoiesis via *JARID2* modulation (**Figure 7B**). Overall, this interaction could explain the MK hyperplasia observed in BM biopsies of PMF patients[19] and the high proliferative potential of MKs derived from PMF CD34+ cells reported in studies *in vitro*[46]. Moreover, the analysis of miR-155-5p and *JARID2* mRNA levels in ET CD34+ cells revealed that this regulatory axis specifically works in PMF CD34+ cells (see **Figure S3** and Supplemental Results).

Taken together, integration of GEP and miEP uncovered regulatory networks in which aberrantly expressed miRNAs and genes interact, thereby elucidating some of the

pathogenetic characteristics of PMF. Finally, integrative analysis has proven to be a good approach for identifying reliable mRNA/miRNA interactions that could contribute to PMF pathogenesis, such as the *JARID2*-miR-155-5p axis, which is involved in hyperplastic megakaryopoiesis.

AUTHORSHIP CONTRIBUTIONS

AMV and RM designed the study; PG, VR, DP, CB, SSalm, GB, MC, AR, and AMV enrolled patients; RZ, RN, VP and TF performed and analyzed microarray and real time-PCR data; PG, CM and TF performed ELISA assays; RZ, RN, VP, AB, SB and ET performed data analysis; VP, SS, GS, ZP, and SR performed gene silencing and miRNA overexpression experiments, RN, EB, SR and SRo carry out luciferase reporter assays. RZ, RN, VP, ET, SF, AMV and RM wrote the manuscript.

CONFLICT OF INTEREST DISCLOSURES

The authors declare no competing financial interests

REFERENCES

1.   Vannucchi AM, Guglielmelli P, Tefferi A. Advances in understanding and management of myeloproliferative neoplasms. *CA Cancer J Clin*. 2009;59(3):171-191.

2.   Tefferi A, Vardiman JW. Classification and diagnosis of myeloproliferative neoplasms: the 2008 World Health Organization criteria and point-of-care diagnostic algorithms. *Leukemia*. 2008;22(1):14-22.

3.   Levine RL, Wadleigh M, Cools J, et al. Activating mutation in the tyrosine kinase JAK2 in polycythemia vera, essential thrombocythemia, and myeloid metaplasia with myelofibrosis. *Cancer Cell*. 2005;7(4):387-397.

4.   Pardanani AD, Levine RL, Lasho T, et al. MPL515 mutations in myeloproliferative and other myeloid disorders: a study of 1182 patients. *Blood*. 2006;108(10):3472-3476.

5.   Vainchenker W, Delhommeau F, Constantinescu SN, Bernard OA. New mutations and pathogenesis of myeloproliferative neoplasms. *Blood*. 2011;118(7):1723-1735.

6.   Vannucchi AM, Lasho TL, Guglielmelli P, et al. Mutations and prognosis in primary myelofibrosis. *Leukemia*. 2013;27(9):1861-1869.

7.   Nangalia J, Massie CE, Baxter EJ, et al. Somatic CALR Mutations in Myeloproliferative Neoplasms with Nonmutated JAK2. *N Engl J Med*. 2013.

8.   Klampfl T, Gisslinger H, Harutyunyan AS, et al. Somatic Mutations of Calreticulin in Myeloproliferative Neoplasms. *N Engl J Med*. 2013.

9.   Chen CZ, Li L, Lodish HF, Bartel DP. MicroRNAs modulate hematopoietic lineage differentiation. *Science*. 2004;303(5654):83-86.

10.   Brennecke J, Hipfner DR, Stark A, Russell RB, Cohen SM. bantam encodes a developmentally regulated microRNA that controls cell proliferation and regulates the proapoptotic gene hid in Drosophila. *Cell*. 2003;113(1):25-36.

11.   Cheng AM, Byrom MW, Shelton J, Ford LP. Antisense inhibition of human miRNAs and indications for an involvement of miRNA in cell growth and apoptosis. *Nucleic Acids Res*. 2005;33(4):1290-1297.

12.   Lee RC, Feinbaum RL, Ambros V. The C. elegans heterochronic gene lin-4 encodes small RNAs with antisense complementarity to lin-14. *Cell*. 1993;75(5):843-854.

13.   Gordon JE, Wong JJ, Rasko JE. MicroRNAs in myeloid malignancies. *Br J Haematol*. 2013;162(2):162-176.

14.   Iorio MV, Croce CM. MicroRNA dysregulation in cancer: diagnostics, monitoring and therapeutics. A comprehensive review. *EMBO Mol Med*. 2012;4(3):143-159.

15.   Guglielmelli P, Tozzi L, Pancrazzi A, et al. MicroRNA expression profile in granulocytes from primary myelofibrosis patients. *Exp Hematol*. 2007;35(11):1708-1718.

16.   Slezak S, Jin P, Caruccio L, et al. Gene and microRNA analysis of neutrophils from patients with polycythemia vera and essential thrombocytosis: down-regulation of micro RNA-1 and -133a. *J Transl Med*. 2009;7:39.

17.   Lin X, Rice KL, Buzzai M, et al. miR-433 is aberrantly expressed in myeloproliferative neoplasms and suppresses hematopoietic cell growth and differentiation. *Leukemia*. 2013;27(2):344-352.

18.   Zhan H, Cardozo C, Yu W, et al. MicroRNA deregulation in polycythemia vera and essential thrombocythemia patients. *Blood Cells Mol Dis*. 2013;50(3):190-195.

19.   Vardiman JW, Thiele J, Arber DA, et al. The 2008 revision of the World Health Organization (WHO) classification of myeloid neoplasms and acute leukemia: rationale and important changes. *Blood*. 2009;114(5):937-951.

20.   Guglielmelli P, Barosi G, Specchia G, et al. Identification of patients with poorer survival in primary myelofibrosis based on the burden of JAK2V617F mutated allele. *Blood*. 2009;114(8):1477-1483.

21.   Salati S, Zini R, Bianchi E, et al. Role of CD34 antigen in myeloid differentiation of human hematopoietic progenitor cells. *Stem Cells*. 2008;26(4):950-959.

22. Zini R, Norfo R, Ferrari F, et al. Valproic acid triggers erythro/megakaryocyte lineage decision through induction of GFI1B and MLLT3 expression. *Exp Hematol*. 2012;40(12):1043-1054 e1046.

23. Tenedini E, Roncaglia E, Ferrari F, et al. Integrated analysis of microRNA and mRNA expression profiles in physiological myelopoiesis: role of hsa-mir-299-5p in CD34+ progenitor cells commitment. *Cell Death Dis*. 2010;1:e28.

24. Guglielmelli P, Zini R, Bogani C, et al. Molecular profiling of CD34+ cells in idiopathic myelofibrosis identifies a set of disease-associated genes and reveals the clinical significance of Wilms' tumor gene 1 (WT1). *Stem Cells*. 2007;25(1):165-173.

25. Schotte D, Pieters R, Den Boer ML. MicroRNAs in acute leukemia: from biological players to clinical contributors. *Leukemia*. 2012;26(1):1-12.

26. Deng H, Guo Y, Song H, et al. MicroRNA-195 and microRNA-378 mediate tumor growth suppression by epigenetical regulation in gastric cancer. *Gene*. 2013;518(2):351-359.

27. Li H, Zhao H, Wang D, Yang R. microRNA regulation in megakaryocytopoiesis. *Br J Haematol*. 2011;155(3):298-307.

28. O'Connell RM, Zhao JL, Rao DS. MicroRNA function in myeloid biology. *Blood*. 2011;118(11):2960-2969.

29. Ramirez-Herrick AM, Mullican SE, Sheehan AM, Conneely OM. Reduced NR4A gene dosage leads to mixed myelodysplastic/myeloproliferative neoplasms in mice. *Blood*. 2011;117(9):2681-2690.

30. Yang L, Wang L, Kalfa TA, et al. Cdc42 critically regulates the balance between myelopoiesis and erythropoiesis. *Blood*. 2007;110(12):3853-3861.

31. Puda A, Milosevic JD, Berg T, et al. Frequent deletions of JARID2 in leukemic transformation of chronic myeloid malignancies. *Am J Hematol*. 2011;87(3):245-250.

32. Nemeth MJ, Kirby MR, Bodine DM. Hmgb3 regulates the balance between hematopoietic stem cell self-renewal and differentiation. *Proc Natl Acad Sci U S A*. 2006;103(37):13783-13788.

33. Bianchi E, Zini R, Salati S, et al. c-myb supports erythropoiesis through the transactivation of KLF1 and LMO2 expression. *Blood*. 2010;116(22):e99-110.

34. Hussein K, Theophile K, Dralle W, Wiese B, Kreipe H, Bock O. MicroRNA expression profiling of megakaryocytes in primary myelofibrosis and essential thrombocythemia. *Platelets*. 2009;20(6):391-400.

35. Rampal R, Al-Shahrour F, Abdel-Wahab O, et al. Integrated genomic analysis illustrates the central role of JAK-STAT pathway activation in myeloproliferative neoplasm pathogenesis. *Blood*. 2014;123(22):e123-133.

36. Barbui T, Finazzi G, Falanga A. Myeloproliferative neoplasms and thrombosis. *Blood*. 2013;122(13):2176-2184.

37. Konopleva M, Mikhail A, Estrov Z, et al. Expression and function of leptin receptor isoforms in myeloid leukemia and myelodysplastic syndromes: proliferative and anti-apoptotic activities. *Blood*. 1999;93(5):1668-1676.

38. Dos Santos C, McDonald T, Ho YW, et al. The Src and c-Kit kinase inhibitor dasatinib enhances p53-mediated targeting of human acute myeloid leukemia stem cells by chemotherapeutic agents. *Blood*. 2013;122(11):1900-1913.

39. Shpilman M, Niv-Spector L, Katz M, et al. Development and characterization of high affinity leptins and leptin antagonists. *J Biol Chem*. 2011;286(6):4429-4442.

40. Tokuhisa Y, Lidsky ME, Toshimitsu H, et al. Src Family Kinase Inhibition as a Novel Strategy to Augment Melphalan-Based Regional Chemotherapy of Advanced Extremity Melanoma. *Ann Surg Oncol*. 2013.

41. Lemoli RM, Salvestrini V, Bianchi E, et al. Molecular and functional analysis of the stem cell compartment of chronic myelogenous leukemia reveals the presence of a CD34- cell population with intrinsic resistance to imatinib. *Blood*. 2009;114(25):5191-5200.

42.   Ameres SL, Zamore PD. Diversifying microRNA sequence and function. *Nat Rev Mol Cell Biol*. 2013;14(8):475-488.

43.   Peng JC, Valouev A, Swigut T, et al. Jarid2/Jumonji coordinates control of PRC2 enzymatic activity and target gene occupancy in pluripotent cells. *Cell*. 2009;139(7):1290-1302.

44.   Kitajima K, Kojima M, Nakajima K, et al. Definitive but not primitive hematopoiesis is impaired in jumonji mutant mice. *Blood*. 1999;93(1):87-95.

45.   O'Connell RM, Rao DS, Chaudhuri AA, et al. Sustained expression of microRNA-155 in hematopoietic stem cells causes a myeloproliferative disorder. *J Exp Med*. 2008;205(3):585-594.

46.   Balduini A, Badalucco S, Pugliano MT, et al. In vitro megakaryocyte differentiation and proplatelet formation in Ph-negative classical myeloproliferative neoplasms: distinct patterns in the different clinical phenotypes. *PLoS One*. 2012;6(6):e21015.

Table 1. DEGs selected by biological significance

Gene Symbol	Gene Ontology function	Notes	FC
ANGPT1	Secreted protein	Overexpressed in AML, CML, MDSs	3,1
ANXA3	Cytoplasmatic protein	Negative prognostic factor for prostate cancer	10,4
ARHGAP18	Cytoplasmatic protein	Involved in cell spreading and motility	3,0
CD9	Membrane protein	Involved in platelet activation and aggregation; involved in BM remodeling in PMF	2,2
CEACAM8	Membrane protein	Overexpressed in imatinib resistant CML cells	5,5
CP	Enzyme	Overexpressed in AML; negative prognostic factor for renal carcinoma	2,6
DEFA1	Secreted protein	Overexpressed in imatinib resistant CML cells; biomarker for diagnosis of CRCA	60,2
FGR	Kinase	Involved in cell migration	1,9
FHL2	Transcription factor	Promotes myeloid proliferation; overexpressed in AML	2,7
IDH1	Cytoplasmatic protein	Mutated in MPNs	2,4
IFI27	Membrane protein	Involved in defense and immunity	2,4
IFIH1	Cytoplasmatic protein	Involved in defense and immunity	2,3
IKZF2	Transcription factor	Overexpressed in in Hodgkin Lymphoma and ALL	3,6
ITGB3	Membrane protein	Involved in platelet activation and aggregation	2,5
LCN2	Secreted protein	Expression induced by BCR-ABL protein; negative prognostic factor for breast cancer	7,0
LEPR	Membrane protein	Overexpressed in AML and PMF; involved in fibrosis	9,7
MAF	Transcription factor	Negative prognostic factor for MM	8,0
MEF2C	Transcription factor	Involved in MKs differentiation	2,3
MMP9	Extracellular matrix protein	Involved in the development of fibrosis	3,8
MYC	Transcription factor	Involved in MKs differentiation, cancer marker	2,8
NFE2	Transcription	Involved in MKs differentiation; overexpressed in PMF	2,0

		factor	
OLFM4	Secreted protein	Negative prognostic factor for colorectal, breast and lung cancer	3,5
PF4	Secreted protein	Involved in platelet activation and aggregation	3,4
PIM1	Transcription factor	Overexpressed in PMF	2,6
RHOB	Cytoplasmatic protein	Involved in cell spreading and motility	3,7
TIMP3	Extracellular matrix protein	Involved in the development of fibrosis	4,0
TM4SF1	Membrane protein	Involved in cell spreading and motility	4,4
VWF	Secreted protein	Highly expressed by early MKs, involved in platelet adhesion	4,4
WT1	Transcription factor	Negative prognostic factor in AML; associated with high severity score in PMF	2,0
AFF3	Transcription factor	Fusion with MLL gene in ALL and with RUNX1 gene, partner of MLL	-2,2
ARHGEF7	Cytoplasmatic protein	Involved in cell migration, attachment and cell spreading	-2,2
ARID4A	Nuclear protein	Involved in chromatin remodeling; K/O mice develop myelofibrosis	-2,3
BRWD1	Nuclear protein	Involved in chromatin remodeling	-1,8
CDC42	Cytoplasmatic protein	Cdc42-deficient mice developed a fatal myeloproliferative disorder	-4,9
CEBPD	Transcription factor	Myeloid commitment regulator	-2,2
CEBPG	Transcription factor	Myeloid commitment regulator	-2,5
CXCR4	Membrane protein	Involved in bone marrow homing	-2,5
EIF2AK3	Kinase	The ablation in tumor cells resultes in accumulation of ROS	-3,0
FOXO1	Transcription factor	Involved in OXS response; negative prognostic factor for AML	-2,3
HMGB3	Nuclear protein	Involved in chromatin remodeling; required for the proper balance between HSC self-renewal and differentiation	-2,5
IRF4	Transcription factor	Downregulated in CML	-2,7
IRF8	Transcription factor	Downregulated in CML	-6,4

JARID2	Nuclear protein	Involved in chromatin remodeling and in AML progression	-2,5
KLF3	Transcription factor	Downregulated in AML; K/O mice display abnormalities in hematopoiesis	-3,6
MAFF	Transcription factor	Myeloid commitment regulator	-2,0
MEF2D	Transcription factor	Involved in myogenic differentiation; fusion with DAZAP1 gene in ALL	-2,7
MLL5	Transcription factor	Frequently deleted in human myeloid malignancies	-2,7
MXD1	Transcription factor	Involved in regulation of cell proliferation; antagonizes MYC gene	-3,4
NR4A3	Nuclear protein	Involved in chromatin remodeling; hypoallelic mice display MDS/MPNs feeatures	-2,4
NUP98	Transcription factor	Involved in fusions with different partner genes in patients with hematopoietic malignancies	-2,5
PHC3	Nuclear protein	Component of polycomb repressive complex	-2,1
PURB	Nuclear protein	Deleted in MDS and AML	-2,5
RUNX2	Transcription factor	Involved in hematopoietic and osteogenic lineages differentiation	-2,1
SF3B1	Nuclear protein	Mutated in MDS and in MDS/MPNs	-2,0
SMAD7	Transcription factor	Involved in fibrosis; downregulated in MDSs	-7,2
TCF4	Transcription factor	Myeloid commitment regulator	-2,4
TLE4	Transcription factor	Deleted in AML	-2,2
TP53INP1	Nuclear protein	Loss of expression in several cancers; inactivation correlates with increased cell migration	-2,5

Abbreviations: AML, acute myeloid leukemia; CML, chronic myeloid leukemia; MDSs, myelodysplastic syndromes; BM, bone marrow; PMF, primary myelofibrosis; ALL, acute lymphoblastic leukemia; CRCA, colorectal cancer; MPNs, myeloproliferative neoplasms; MM, multiple myeloma; MKs, megakaryocytes; K/O, knock/out; ROS, reactive oxygen species; OXS, oxidative stress; HSC, hematopoietic stem cell; MDS/MPNs, myelodysplastic/myeloproliferative neoplasms

FIGURE LEGENDS

Figure 1. Principal component analysis (PCA) of gene and microRNA expression microarray data. (A) The PCA graph of global gene expression data and (B) PCA graph of global miRNA expression data were computed using Partek GS, version 6.6; bone marrow (BM) control samples are shown as red spheres; peripheral blood (PB) control samples are shown as blue spheres; primary myelofibrosis (PMF) samples are shown in green. PMF JAK2 wild-type samples are shown as pyramids, while PMF JAK2V617F samples are shown as prisms.

Figure 2. Validation of the selected genes and miRNAs in granulocytes and plasma from primary myelofibrosis (PMF) patients. (A) Expression of the seven selected genes in granulocytes from PMF patients and healthy donors. Gene expression levels were measured by quantitative reverse transcription polymerase chain reaction (qRT-PCR) starting from granulocyte total RNA and were expressed as relative quantity (RQ). Boxes represent the interquartile range that contains 50% of the subjects, the horizontal line in the box marks the median, and the bars show the range of values. Data are representative of 32 PMF and 12 control (CTR) samples. (B) Serum levels of two secreted proteins (LCN2 and OLFM4) in PMF patients and healthy donors. Protein levels were measured by enzyme-linked immunosorbent assay (ELISA) and were expressed as ng/mL. Boxes represent the interquartile range that contains 50% of the subjects, the horizontal line in the box marks the median, and the bars show the range of values. Data are representative of 30 PMF and 8 CTR samples. (C) Expression levels of the eight selected miRNAs in granulocytes from PMF patients and healthy donors. The miRNA expression levels were measured by qRT-PCR starting from granulocyte total RNA and were expressed as RQ. Boxes represent the interquartile range that contains 50% of the subjects, the horizontal line in the box marks the median, and the bars show the range of values. Data are representative of 32 PMF and 12 CTR samples. *, $P < .05$ vs. CTR.

Figure 3. Regulatory networks of mRNA-miRNA interactions built through Ingenuity Pathway Analysis (IPA). Visualization of the regulatory networks enriched for: (A) chromatin remodeling genes, (B) myeloid transcription factors, and (C) myeloproliferative disorder-related genes. Red filling means upregulation, while green filling indicates downregulation.

Figure 4. Validation of 3´UTR–miRNA interactions. (A) Normalized luciferase activity of K562 cells nucleofected with the indicated miRNA mimics and 3'untranslated region (3´UTR) luciferase reporter vectors. Firefly luciferase activity was measured 48 h after nucleofection and normalized to *Renilla* luciferase activity. Values are reported as mean ± standard error of the mean (SEM); *, $P < .05$ versus miRNA mimic negative control (Neg-mimic). Results come from three independent experiments performed in duplicate. (B) Graphical representation of mRNA-miRNA interactions validated by means of 3´UTR luciferase reporter assays. Solid lines (validated interactions); dashed lines (not validated interactions). (C) Results of the luciferase reporter assays performed with wild type and mutant 3'UTR. Assays were carried out only for the 3'UTR-miRNA interactions previously validated (see panel A). Each bar represents the luciferase activity upon miRNA overexpression normalized on the value of the same 3'UTR luciferase vector upon Neg-mimic transfection. Values are reported as mean ± SEM; *, $P < .05$ versus mutant 3'UTR. Results come from three independent experiments performed in duplicate.

Figure 5. Effect of JARID2 silencing on normal CD34+ cell differentiation. (A) Expression levels of *JARID2* at 24 and 48 h after the last nucleofection were measured by qRT-PCR and data are reported as RQ. (B–C) Results of the statistical analysis on the percentage of CD41+ cells performed by flow cytometry at day 5, 8, 10, and 12 after the last nucleofection on serum-free multilineage and megakaryocyte (MK) unilineage cultures. (D) Results of the statistical analysis of collagen-based clonogenic assay. The cells were plated 24 h after the last nucleofection and scored after 12 days. (E) Morphological analysis of negative control (NegCTR) (i–ii) and *JARID2*- short interfering RNA (*JARID2*-siRNA) (iii–iv) samples after May–Grünwald–Giemsa staining at day 8 and 10 of MK unilineage culture after the last nucleofection in a representative experiment. Magnification, ×1000. Values are reported as mean ± standard error of the mean (SEM). **, $P < .01$ versus NegCTR; *, $P < .05$ versus NegCTR. The results come from five independent experiments. Abbreviations: NegCTR, siRNA negative control; siRNA, small interfering RNA; h, hours; CFU, colony-forming unit.

Figure 6. **Transfection of miR155-5p mimic and inhibitor in normal and PMF CD34+ cells.** (A) Effect of miR155-5p mimic transfection on normal CD34+ cell differentiation. (i) Expression levels of *JARID2* at 24 and 48 h after the last nucleofection, measured by qRT-

PCR and reported as RQ. (ii-iii) Results of statistical analysis on the percentage of CD41+ cells performed by flow cytometry at day 5, 8, 10, and 12 after the last nucleofection on serum-free multilineage and MK unilineage cultures. (iv) Results of the statistical analysis of the collagen-based clonogenic assay. The cells were plated 24 h after the last nucleofection and scored after 12 d. (v) Morphological analysis of Neg-mimic and miR-155-5p nucleofected cells after May–Grünwald–Giemsa staining at days 8 and 10 of MK unilineage serum-free liquid culture after the last nucleofection in a representative experiment. Magnification ×1000. Values are reported as mean ± standard error of the mean (SEM). **, $P < .01$ versus Neg-mimic; *, $P < .05$ versus Neg-mimic. The results come from five independent experiments. (B) Effect of miR155-5p downregulation in PMF CD34+ cells. (i) Expression levels of *JARID2* in PMF CD34+ cells at 24 and 48 h after the last nucleofection of miR-155-5p inhibitor. The *JARID2* expression was measured by qRT-PCR and data are reported as RQ. (ii-iii) Percentage of viable CD41+ cells assessed by flow cytometry at day 5, 8, and 10 after the last nucleofection on serum-free multilineage and MK unilineage cultures. (iv) Results of the statistical analysis of the collagen-based clonogenic assay. The cells were plated 24 h after the last nucleofection and scored after 12 d. (v) Morphological analysis of negative control inhibitor (NegINH) and miR-155-5p inhibitor treated cells after May–Grünwald–Giemsa staining at days 8 and 10 of MK unilineage serum-free liquid culture after the last nucleofection in a representative experiment. Magnification ×1000. Values are reported as mean ± SEM. **, $P < .01$ versus Neg-INH; *, $P < .05$ versus Neg-INH. The results come from four independent experiments. Abbreviations: Neg-mimic, miRNA mimic Negative Control; h, hours; CFU, colony-forming unit; Neg-INH, miRNA inhibitor Negative Control.

Figure 7. **Simultaneous overexpression or inhibition of *JARID2* and miR-155-5p in normal CD34+ cells.** (A) Rescue of *JARID2* expression in miR-155-5p overexpressing cells. (i) Flowchart listing the experiment timing (expressed in days) after NGFR+ cell purification. (ii) Expression levels of *JARID2* in CB CD34+ cells after NGFR+ cells purification. The *JARID2* expression was measured by qRT-PCR and data are reported as RQ. (iii) Percentage of viable CD41+ cells in the MK unilineage culture assessed by flow cytometry at day 4, 7, and 11 after NGFR+ cell purification. (iv) Results of the statistical analysis of the collagen-based clonogenic assay. The cells were plated 24 h after NGFR+ cell purification and scored after 12 d. Values are reported as mean ± standard error of the mean (SEM). **, $P < .01$; *, $P < .05$. The results come from three independent

27

experiments. (B) Simultaneous downregulation of *JARID2* and miR155-5p in CB CD34+ cells. (i) Flowchart reporting the experiment timing (expressed in days) after the last nucleofection. (ii) Expression levels of JARID2 in CB CD34+ cells at 48 h after the last nucleofection. The JARID2 expression was measured by qRT-PCR and data are reported as RQ. (iii) Percentage of viable CD41+ cells in the MK unilineage culture assessed by flow cytometry at day 8, 10, and 12 after the last nucleofection. (iv) Results of the statistical analysis of the collagen-based clonogenic assay. The cells were plated 24 h after the last nucleofection and scored after 12 d. Values are reported as mean ± SEM. **, $P < .01$; *, $P < .05$. The results come from three independent experiments. Abbreviations: Neg-mimic, miRNA mimic Negative Control; h, hours; CFU, colony-forming unit; NegCTR, siRNA negative control; NegINH, miRNA inhibitor Negative Control.

A

B

Disease		V617F JAK2
■ BM CTR		● ND
■ PB CTR		● V617F
■ PMF		▲ wild type
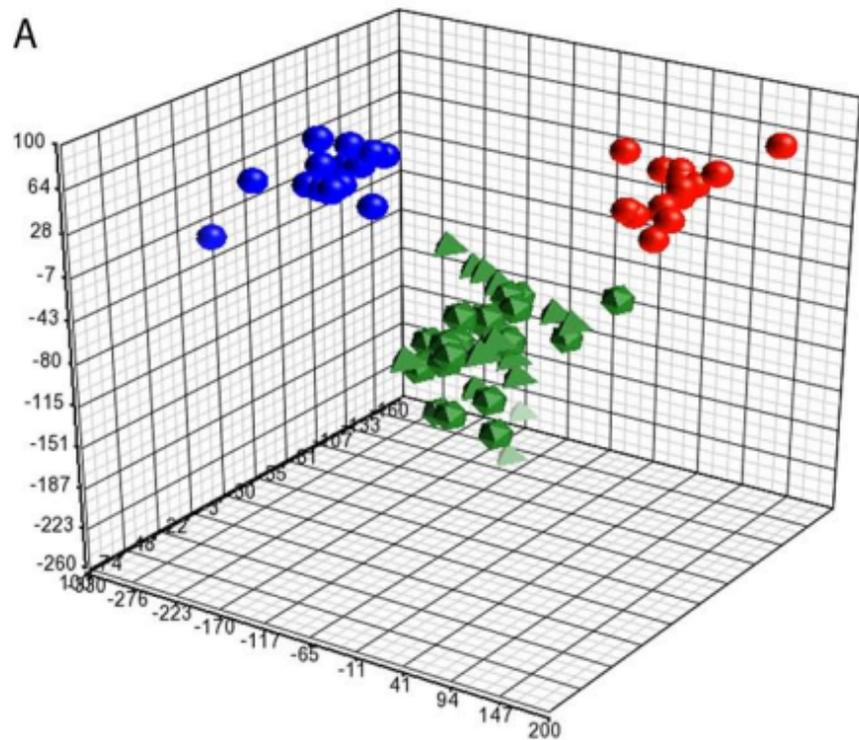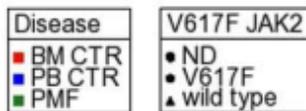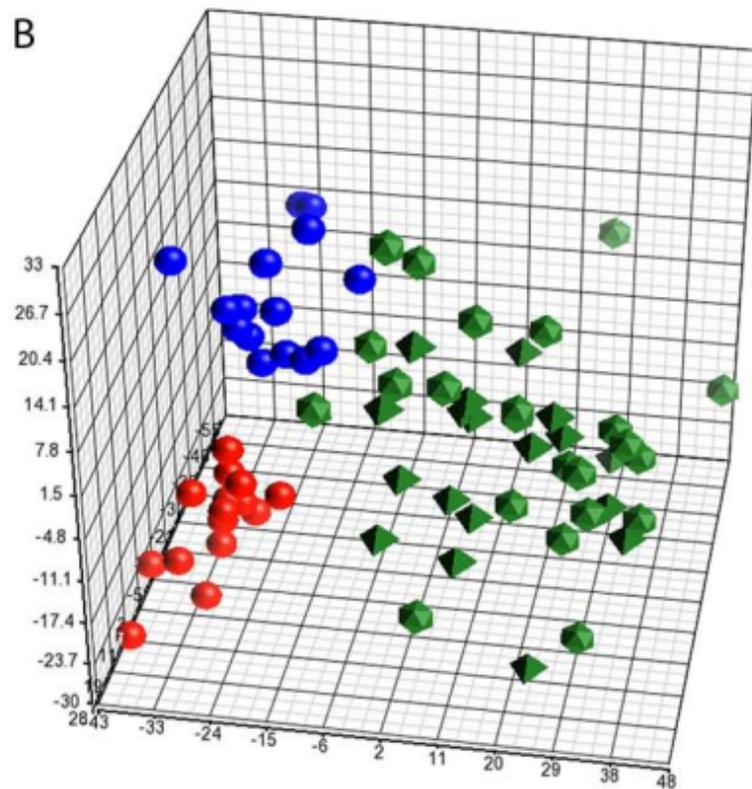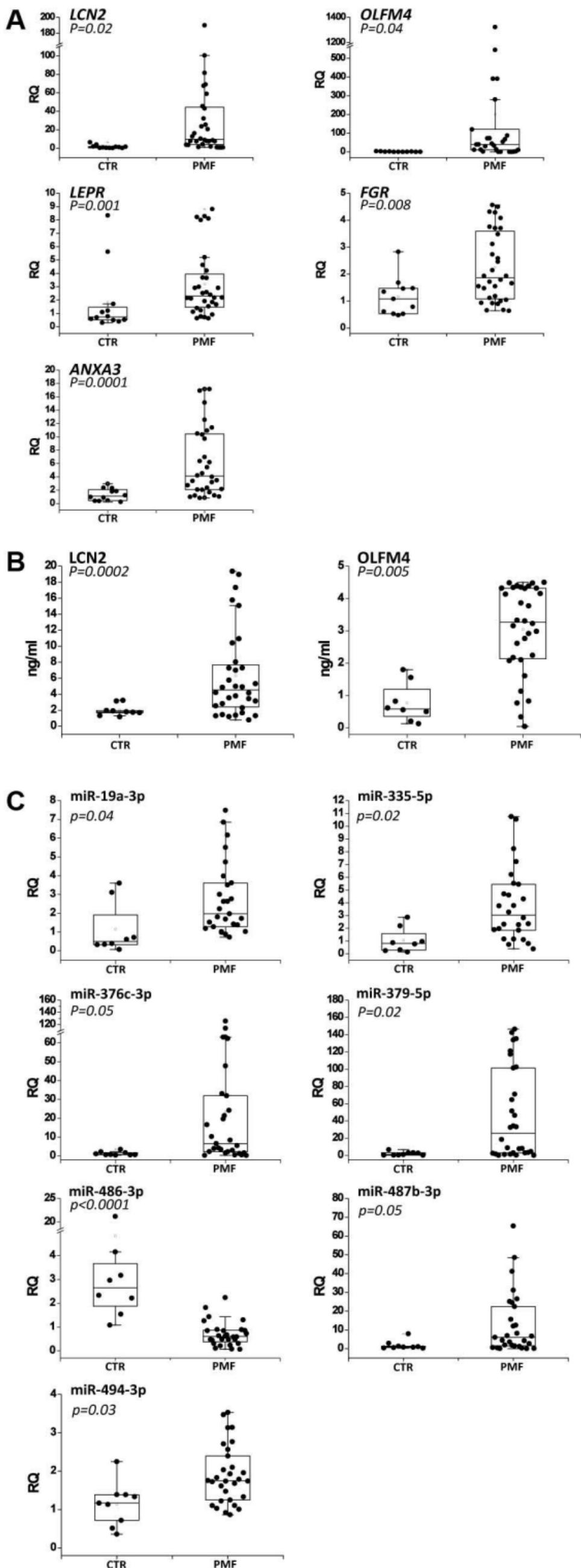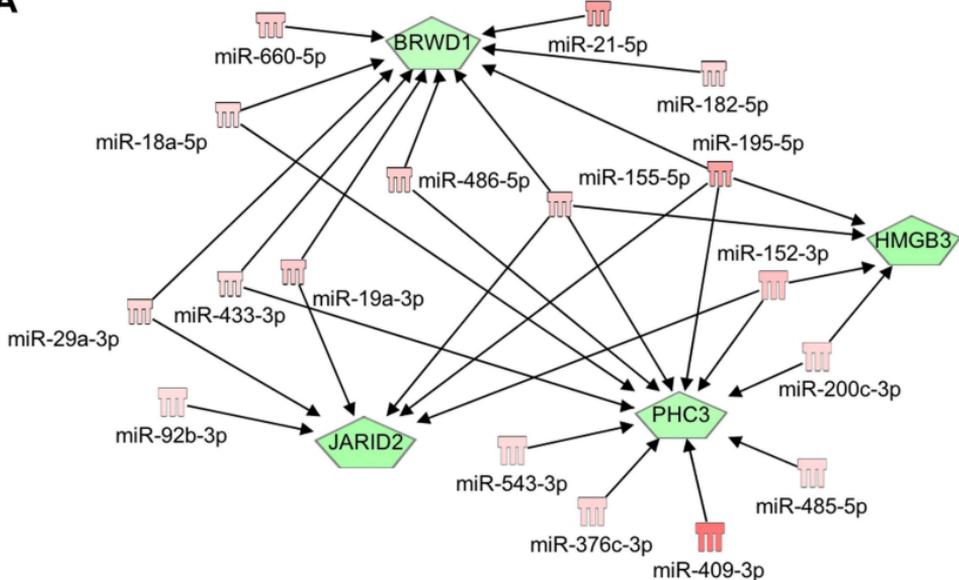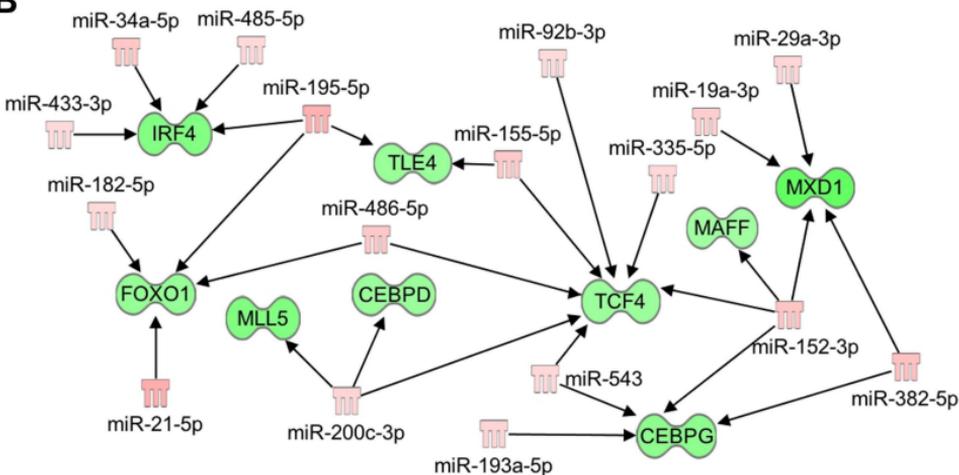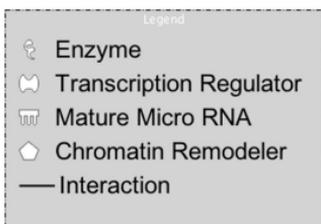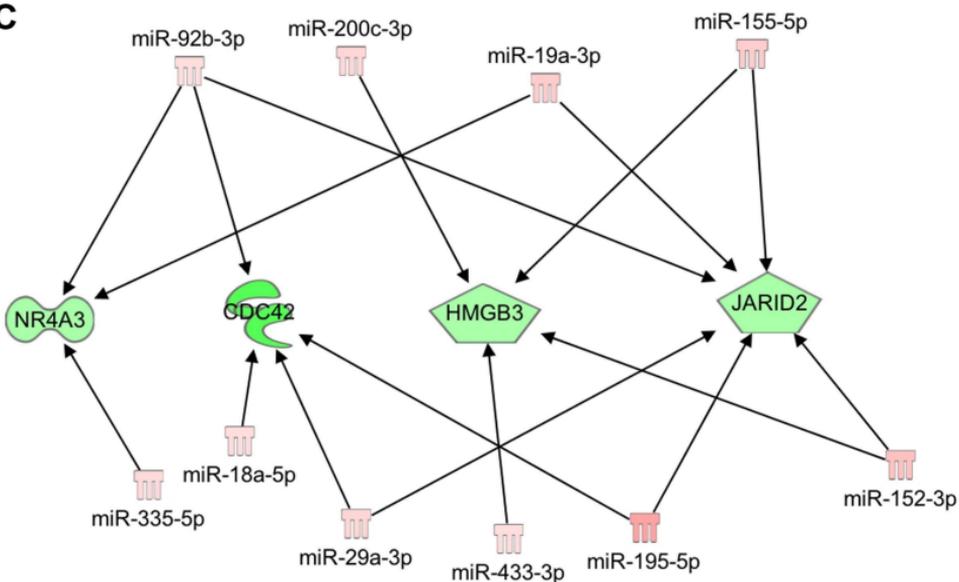
Figure 1
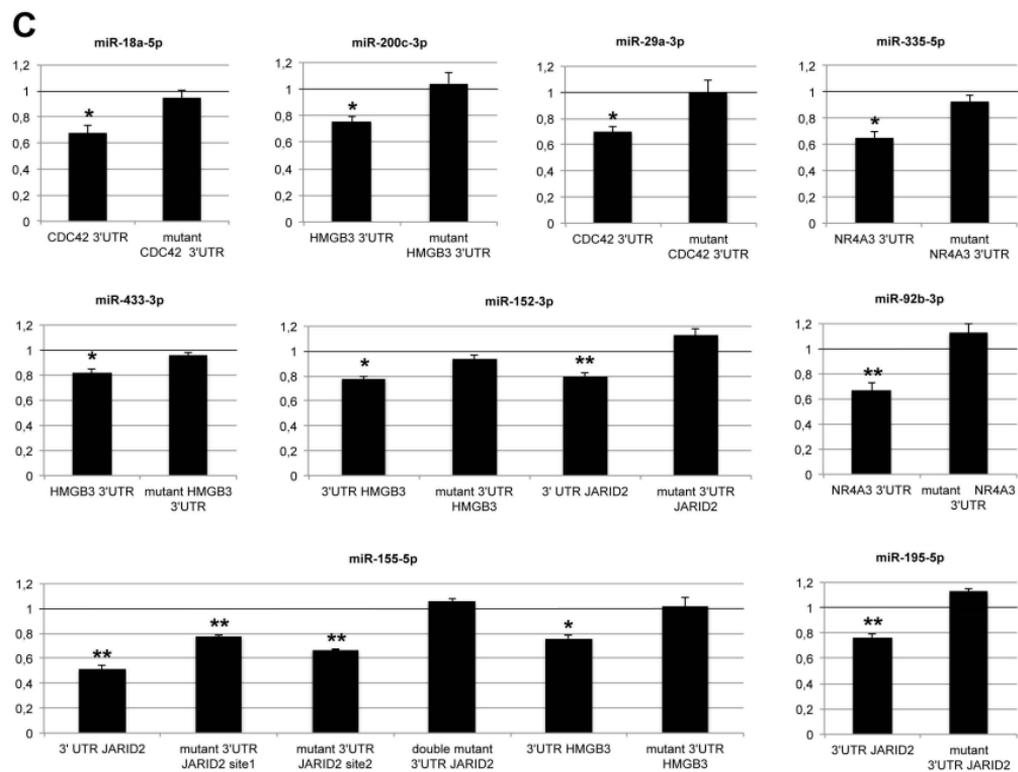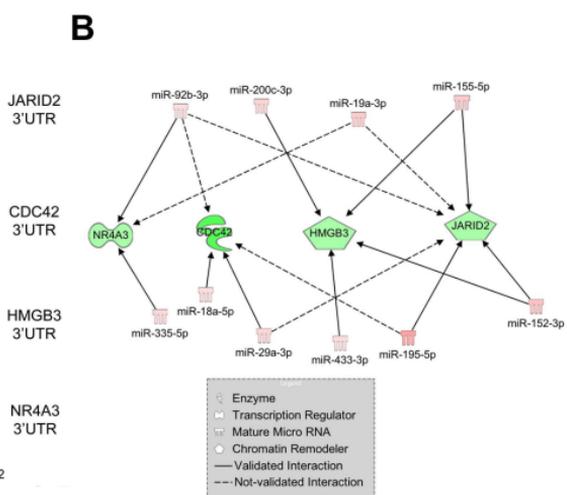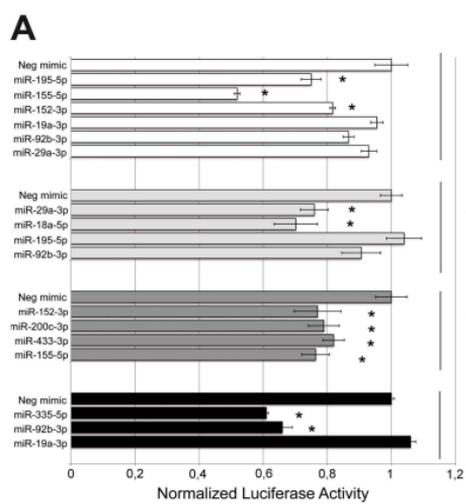
Figure 2

Figure 3

Figure 4

Figure 5

Figure 6

Figure 7